AD-A068 184 WASHINGTON UNIV SEATTLE DEPT OF MECHANICAL ENGINEERING F/G 11/6
DYNAMIC ANALYSES OF HOMALITE-100 AND POLYCARBONATE MODIFIED COM--ETC(U)
MAR 79 A S KOBAYASHI, K SEO, J Y JOU, Y URABE N00014-76-C-0060

UNCLASSIFIED TR-35 NL

| OF |
AD
A068184

END
DATE
FILMED
7--79
DDC

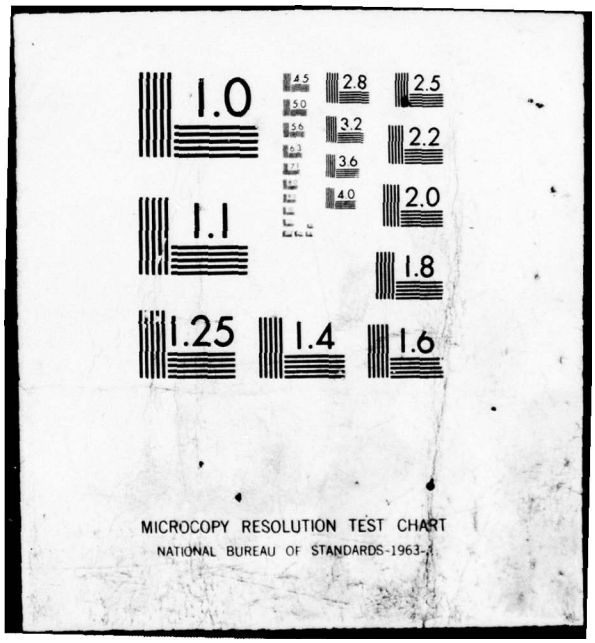
1.0
1.1
1.25
1.4
1.6
1.8
2.0
2.2
2.5
2.8
3.2
3.6
4.0
4.5
5.0
5.6
6.3
MICROCOPY RESOLUTION TEST CHART
NATIONAL BUREAU OF STANDARDS-1963-A

LEVEL II

12 B.S.

Office of Naval Research

Contract N00014-76-C-0060 NR 064-478

Technical Report No. 35

DYNAMIC ANALYSES OF HOMALITE-100 AND POLYCARBONATE MODIFIED COMPACT-TENSION SPECIMENS

by

A.S. Kobayashi, K. Seo, J.Y. Jou and Y. Urabe

March 1979

The research reported in this technical report was made possible through support extended to the Department of Mechanical Engineering, University of Washington, by the Office of Naval Research under Contract N00014-76-C-0060 NR 064-478. Reproduction in whole or in part is permitted for any purpose of the United States Government.

Department of Mechanical Engineering

College of Engineering

University of Washington

ABSTRACT

The fracture dynamic and crack arrest responses of modified compact tension specimen (M-CT) machined from Homalite-100 and polycarbonate sheets were studied by dynamic photoelasticity, dynamic finite element analysis and streaking photography. In contrast to the results of a previous study involving a mild steel M-CT specimen, substantial dynamic effects were observed during crack propagation in the Homalite-100 and polycarbonate M-CT specimens. Although the crack arrest toughnesses, K_{Ia}, were within 10 percent of the corresponding static stress intensity factor at crack arrest, their values were about 80 percent and 50 percent of the corresponding fracture toughness, K_{IC}, of Homalite-100 and polycarbonate, respectively.

INTRODUCTION

In a recent paper, two of the authors used a dynamic finite element code to compute the dynamic fracture toughness of a fracturing transverse wedge-loaded, modified compact tension (M-CT) specimen machined from AISI 1018 steel [1]. The dynamic finite element code, HONDO [2], was used in its "generation phase" [3] where the crack was driven by the experimentally determined crack motion and the associated dynamic fracture toughness, K_{ID}, was calculated. This singular result involving a very ductile material with a notched brittle weld starter crack [4], lead to the conclusion that little difference between the dynamic and static stress intensity factors existed in the particular M-CT specimen analyzed. This result was not only in disagreement with all previously obtained results for different specimen geometries [5] but also contradicted the analytical-experimental results obtained by Hahn et al. [6] for a similar M-CT specimens but with different crack starter. Although a valid plane strain fracture toughness, K_{IC}, for the mild steel M-CT specimen analyzed in Reference [2] was not available, the

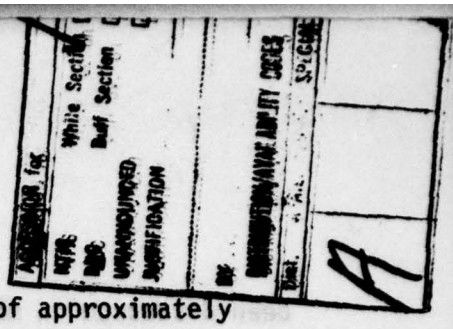

calculated crack arrest stress intensity factor, K_{Ia}, of approximately 88 $MP_a\sqrt{M}$ (80 ksi $\sqrt{in}$) would have been considerably lower than such fracture toughness and was not consistent with the photoelastic results obtained for Homalite-100 M-CT specimens by T. Kobayashi et al. [7] where K_{Ia} was nearly equal to the K_{IC} = 445 KPa$\sqrt{M}$ (405 psi $\sqrt{in}$).

Since similar differences between K_{IC} and K_{Ia} were observed in dynamic tear (DT) specimens machined from the relatively brittle Homalite-100 and the ductile polycarbonate plates [8,9], it is thought that the influence of ductibility could be delineated if comparative fracture dynamic studies were conducted on M-CT specimens machined from Homalite-100 and polycarbonate plates. As a result, a combined experimental-numerical analyses of M-CT specimens machined from Homalite-100 and polycarbonate were conducted and reported in this paper.

The M-CT specimens, as shown in the legend of Figure 1, are full-size models of the dynamic fracture specimen being investigated in a current ASTM E24.03.04 Subcommittee on Dynamic Testing, Dynamic Initiation-Crack Arrest Task Group [10]. The experimental and numerical procedures used in this study were the now popular dynamic photoelasticity [7,8,9] and the dynamic finite element method [8,9] used in its generation phase [3], respectively. In three experiments, crack velocity measurements, which were in the past obtained by discrete crack length measurements and the timing marks from a Lite-Mike, were also obtained from continous crack length recording using a streaking camera.

EXPERIMENTAL PROCEDURES

Dynamic Photoelasticity

The 16-spark gap Cranz-Schardin camera and the associated dynamic photoelasticity system, which was originally developed by Riley and Dally [11], has

been discussed in many previous publications and thus will not be repeated here. Figure 2 shows two typical dynamic photoelastic patterns surrounding a running crack tip in a polycarbonate M-CT specimen. The two polycarbonate M-CT specimens of 6.4 mm (1/4 in.) thickness, which were analyzed by dynamic photoelasticity, were annealed at 160°C overnight to eliminate residual stresses. A starter crack of approximately 2.5 mm (1/4 in.) length was sawed and chiseled from the tip of the machined notch. The blunt starter crack initiated crack propagation at a relatively high crack initiation fracture toughness, K_{IQ}, and thus propagated the crack nearly through the entire width of the specimen. The average mechanical and optical properties used in photoelastic data reduction as well as in dynamic finite element analyses are identical to those listed in Reference [9].

Errors in K_{ID} Determination

When dynamic photoelasticity is used for fracture dynamic analysis, the transient dynamic isochromatic lobes surrounding the running crack tip must be related to an instantaneous dynamic stress intensity factor. Following the original suggestion by Irwin [12], normally this conversion is made by using either one, two [13,14] or multiple terms [15,16] in the static crack-tip stresses of Williams eigenfunction [17].

Errors involved in using the above static near-field state of stress were later assessed by Kobayashi and Mall [18] who used the dynamic counterpart [19] of Williams stress function to show that overestimations of 10 percent or more in dynamic stress intensity factor were possible at a relative slow crack velocity, $\dot{a}$, of 15 percent of the dilatational wave velcoty, i.e. $0.15c_1$, and that such error increased with the use of larger dynamic isochromatic lobes. Reference [18] also showed that stress waves propagating in the vicinity of the crack tip could distort the dynamic isochromatic lobes and could induce additional errors in

dynamic stress intensity factor determination. Such stress waves could be a visible rectangular pulse as recorded photoelastically by Wade and Kobayashi [20] or an innocuous ramp pulse which is about to impact the propagating crack tip.

As a result of possible compounded errors involved in the use of statis stress field to characterize a dynamic phenomena and from the not-so-apparent stress wave interactions with the propagating crack tip, the authors have used the smallest visible isochromatic lobe, prefereably within 2.5 mm (0.1 in.) distance from the moving crack tip, to extract the dynamic stress intensity factor at higher crack velocities. Such size restriction on the permissible isochromatic lobe unfortunately taxes the exprimental accuracies in determining the size of the isochromatic lobe as well as the instantaneous location of the crack tip. This limited resolution in K_{ID} determination via dynamic photoelasticity, which is estimated to be at the best ± 5 percent, is akin to the corresponding limitation in dynamic finite element analysis when used for dynamic fracture analysis.

Crack Velocity Measurements

In a previous paper [18], the authors discussed the experimental errors involved in measuring the crack tip motion and the need to smooth the raw data to confine the experimental scatter in the K_{ID} versus $\dot{a}$ relation of Reference [21]. Recent numerical experimentation [22] using an upgraded fracture mechanics subroutine in a dynamic finite element code showed that slight perturbations in the crack tip motion, which resulted in mild oscillations in the crack tip velocities, could generate significant osciallations in the calculated K_{ID}.

In order to determine the existence or lack of existence of crack velocity variation during dynamic crack propagation, crack velocities were measured in two Homalite-100 (thickness 9.5 mm) and one polycarbonate M-CT specimens (thickness 6.4 mm) using a Beckman Whitely Model 318 streaking camera.

Figure 3 shows schematically the experimental setup as well as a typical streaking photograph of a fracturing polycarbonate M-CT specimen. Simultaneous dynamic photoelastic recording was not possible because the stray light from the light source for the streaking camera interfered with the Crane-Shardin camera system. The apparent high initial crack velocity from the streaking photograph of Figure 3 is due to the lack of an adequate pre-triggering system for the light source. The estimated crack velocity at the onset of rapid crack propagation was thus extrapolated from the steady state crack velocity as marked in the streaking photography of Figure 3.

Figures 4 and 5 show typical crack velocity relations generated from the crack position versus time relations obtained by the streaking photographs. The crack velocities in the two Homalite-100 and one polycarbonate M-CT specimens exhibited little change during much of the crack propagation.

DYNAMIC FINITE ELEMENT ANALYSIS

The dynamic finite element code which was initially [2] introduced for dynamic fracture analysis in the "generation mode" has undergone substantial changes in the past four years. An improved crack tip release mechanism for rapid crack propagation has been developed and an updated plane stress algorithm for computing dissipation energy at the crack tip has been incorporated. After many numerical experimentations, a linearly varying crack tip nodal release force was found to adequately simulate a more gradual transition of the crack tip movement to its adjacent node [23]. An additional improvement made for this study is an iteration algorithm during each built-in time increment of HONDO [2] to match the applied nodal force with the nodal force calculated from the incremental change in nodal velocity in this explicit dynamic finite element code. Typically, satisfactory convergence of this iteration scheme, as shown

in Figure 6, is obtained on the average within three iterations and thus the computational efficiency of HONDO is still preserved with the added ability to prescribe known nodal force at each time increment.

The dynamic finite element code with the updated fracture mechanic package was used in its generation mode to calculate the dynamic fracture toughness, K_{ID}. Figure 1 shows a typical finite element breakdown of a M-CT specimen used in this study. The prescribed crack tip motions used in these series of generation calculations were obtained either from the streaking photographs of two Homalite-100 and one polycarbonate M-CT specimens or from the discrete crack tip recordings from the sixteen photographs of two polycarbonate M-CT specimens. Also the past practice [8,9] of using dynamic elastic modulus in stress wave propagation was discarded and the static elastic modulus was used throughout all static and dynamic numerical analyses. This procedure follows the conclusion of Schirrer [24] who concluded that the variations in elastic modulus did not affect the stress distribution appreciably but did change the strain distribution around the propagating crack tip. Static mechanical properties of Homalite-100 and polycarbonate specimens were obtained from References [8,9], respectively.

RESULTS

The dynamic fracture toughness, K_{ID}, during crack propagation and arrest in one Homalite-100 and one polycarbonate M-CT specimen are shown in Figures 4 and 5, respectively. K_{ID} results in these figures were generated numerically from the crack tip motion obtained from streaking photography. Also shown in these two figures are the corresponding static stress intensity factors obtained by static finite element analysis. The static K_I results differ with those reported in Reference [1], due to difference in modelling the

applied load in the M-CT specimen, and is in agreement with the corresponding results obtained from compliance calibration [10]. K_{ID} in Homalite-100 and polycarbonate M-CT specimens, both precipitously drop and continue to remain at nearly constant K_{ID} thereafter. The higher static K_I with respect to the dynamic K_{ID} is an indication that much of the released energy during crack propagation in these specimens is dissipated through kinetic energy without being returned to the crack tip for dissipation through fracture energy.

The results of the Homalite-100 M-CT specimen in Figure 4 is in qualitative agreement with the dynamic photoelastic results obtained for a slightly larger Homalite-100 M-CT specimen (of 12.7 mm thickness) in Reference [21]. The low crack arrest toughness, K_{Ia} 0.25 $MP_a\sqrt{M}$ (227 $psi\sqrt{in}$) ∞ was approximately equal to the minimum dynamic fracture toughness K_{Im} in Figure 13 of Reference [8] and is 55 percent of the fracture toughness, $K_{IC} \doteq$ 0.42 $MP_a\sqrt{M}$ (380 psi $\sqrt{in}$). The crack arrest stress intensity factor of $K_{Ia} \doteq$ 1.65 $MP_a\sqrt{M}$ (1500 ksi $\sqrt{in}$) for the polycarbonate M-CT specimen in Figure 5 is nearly one half of the pop-in fracture toughness of K_{IC} = 3.4 $MP_a\sqrt{M}$ (3.1 ksi $\sqrt{in}$).

Figures 7 and 8 show the K_{ID} versus $\dot{a}$ relations obtained by dynamic photoelasticity for two polycarbonate M-CT specimens. Also shown are the K_{ID} generated numerically using the measured crack velocities shown in Figure 9. As discussed in Reference [22], slight irregularities in crack velocity variations with crack extension contributed to the modest differences in computed and experimentally determined dynamic fracture toughness. Considering the idealized elasto-dynamic model used in the dynamic finite element analysis, the agreements between the experimental and numerical results are good.

DISCUSSIONS

The differences between the static and the dynamic stress intensity factors, as shown in Figures 4, 5, 7 and 8 are substantial and do not exhibit the quasi-static response observed in the AISI 1018 M-CT specimen of Reference [1]. The Homalite-100 M-CT specimens in Reference [7] and in this paper, the polycarbonate M-CT specimens of this paper and A533B M-CT specimens of Reference [6] all exhibit a characteristic decrease in K_{ID} followed by a relatively stationary K_{ID} for almost 3/4 of the crack extension prior to crack arrest. The K_{ID} in the mild steel specimen of Reference [1], on the other hand decreased nearly monotonically and closely followed the corresponding static stress intensity factor. This discrepancy between the bulk K_{ID} data and the singular data of Reference [1] could be attributed in part to the highly localized brittle weld starter crack used in the latter. The artificially low K_{IQ}, possibly lower than the K_{IC} of mild steel, of brittle weld crack starter initiated crack propagation under unrealistic low static fracture toughness and was followed by a quasi-static crack propagation. Since the purpose of developing this M-CT specimen is for dynamic testing [10], it can be concluded that the AISI-1018 M-CT specimen with a brittle weld starter crack did not fulfill its intended use.

Figure 10 shows the K_{ID} versus $\dot{a}$ relation obtained from the results of Figures 5, 7 and 8. Superposed on this figure is the averaged K_{ID} versus $\dot{a}$ relation obtained from polycarbonate dynamic tear (DT) specimens [9]. Not only did the K_{ID} versus $\dot{a}$ relation for the M-CT specimen shift slightly towards the lower $\dot{a}$ but appears to reach a lower maximum crack velocity. The latter result is consistent with the corresponding results for Homalite-100 specimens

[5]. On the other hand, the K_{ID} versus $\dot{a}$ relation, which was obtained from Figure 4 for the Homalite-100 M-CT specimen, coincided with that for Homalite-100 DT specimens [8]. The slight difference in K_{ID} versus $\dot{a}$ relations in polycarbonate fracture specimens is in agreement with the results of Kalthoff et al. [25], which are also verified numerically by Hodulak et al. [26].

Figures 11 and 12 show the computed energy partition in a fracturing Homalite-100 and polycarbonate M-CT specimens, respectively. The substantial kinetic energy term in the polycarbonate M-CT specimen in contrast to that in the Homalite-100 specimen and is probably due to the blunt starter crack used in the former. The computed energy for these specimens in Figures 11 and 12 as well as other specimens balance to within 5 percent of total input energy as an indication of the numerical accuracy which can be expected in these analyses.

CONCLUSIONS

1. The K_{ID} variations with crack propagation in the limited number of Homalite-100 and polycarbonate M-CT specimens analyzed are consistent with similar findings by others [6-9].
2. The significant difference in dynamic responses between the mild-steel M-CT specimen with brittle weld starter crack and the Homalite-100 and polycarbonate M-CT specimens requires further investigation.
3. The shift between the K_{ID} versus $\dot{a}$ relations between Homalite-100 M-CT specimens and DT specimens as well as in polycarbonate specimens could be another indication of the geometry and size dependence of the K_{ID} versus $\dot{a}$ relation.

ACKNOWLEDGEMENT

The results of this investigation were obtained in a research contract funded by the Office of Naval Research under contract N00014-76-C0060

NR 064-478. The authors wish to acknowledge gratefully the continuous support and encouragement of Dr. N. R. Perrone of ONR.

REFERENCES

1. Kobayashi, A.S., Urabe, Y., Mall, S., Emery, A.F. and Love, W.J., "Dynamic Finite Element Analyses of Two Compact Specimens," ASME Journal of Engineering Materials and Technology, Vol. 100, Oct. 1978, pp. 402-410.

2. Keys, S.W., "HONDO-A Finite Element Computer Program for the Large Deformation Dynamic Responses of Axisymmetric Solids," Sandia Laboratories Report SLA-74-0039, April 1974.

3. Kanninen, M.F., "A Critical Appraisal of Solution Techniques in Dynamic Fracture Mechanics," Numerical Methods in Fracture Mechanics edited by A.R. Luxmoore and D.R.J. Owen, University College Swansea, Jan. 1978, pp. 612-633.

4. Hahn, G.T., Hoagland, R.G., Marshall, C.W. and Rosenfield, A.R., "Fast Fracture and Crack Arrest Toughness of Reactor Pressure Vessel Steel," a paper presented at ASTM E-24 Symposium on Crack Arrest Methodology and Applications, Philadelphia, Nov. 6-7, 1978.

5. Kobayashi, A.S. and Mall, S., "Rapid Crack Propagation and Arrest in Polymers," Journal of Polymer Engineering and Science, Vol. 19, No. 2, mid-February 1979, pp. 131-135.

6. Hahn, G.T., Corten, H.T., Debel, C.P., Gehlen, P.C., Hoagland, R.G., Kanninen, M.F., Kim, K.S., Marshall, C.W., Popelar, C., Rosenfield, A.R. and Simon, R., "Critical Experiments, Measurements and Analyses to Establish a Crack Arrest Methodology for Nuclear Pressure Vessel Steels," Progress Report, Oct. 1976-Sept. 1977, prepared under U.S. Nuclear Regulatory Commission Contract No. AT(49-24)-0293, NUREG/CR-0057, BMI-1995.

7. Irwin, G.R., Dally, J.W., Kobayashi, T., Fourney, W.L. and Etheridge, J.M., "Photoelastic Studies of Crack Propagation and Crack Arrest," a University of Maryland report prepared under U.S. Nuclear Regulatory Commission Contract No. AT(49-24)-0172, Sept. 1977.

8. Mall, S., Kobayashi, A.S. and Urabe, Y., "Dynamic Photoelastic and Dynamic Finite Element Analysis of Dynamic Tear Test Specimens," Experimental Mechanics, Vol. 18, Dec. 1978, pp. 449-456.

9. Mall, S., Kobayashi, A.S. and Urabe, Y., "Dynamic Photoelastic and Dynamic Finite Element Analyses of Polycarbonate Dynamic Tear Test Specimens," to be published in ASTM STP.

10. "Prospectus for a Cooperative Test Program on Crack Arrest Toughness Measurement," ASTM E24.03.04 Subcommittee on Dynamic Testing, Dynamic Initiation-Crack Arrest Task Group, Dec. 9, 1977.

11. Riley, W.F. and Dally, J.D., "Recording Dynamic Fringe Patterns with a Cranz-Schardin Camera," Experimental Mechanics, Vol. 9, No. 8, Aug. 1969, pp. 27-33N.

12. Irwin, G. R., "Discussion and Authors' Closure of the Paper, 'The Dynamic Stress Distribution Surrounding a Running Crack - A Photoelastic Analysis,'" Proc. of SESA, XVI (1), 153, pp. 93-36.

13. Bradley, W. B. and Kobayashi, A. S., "An Investigation of Propagating Cracks by Dynamic Photoelasticity," Experimental Mechanics, Vol. 10, No. 3, March 1970, pp. 106-113.

14. Kobayashi, T. and Fourney, W. L., "Dynamic Photoelastic Investigations of Crack Propagation," Proc. of 12th Annual Mtg. Soc. Engrg Sci, Univ. of Texas-Austin, Oct. 20-22, 1975, pp. 131-140.

15. Bradley, W. B. and Kobayashi, A. S. "Fracture Dynamics - A Photoelastic Investigation," Engrg Fracture Mechanics, Vol. 3, 1971, pp. 317-332.

16. Etheridge, J. M., Dally, J. W. and Kobayashi, T., "A New Method of Determining the Stress Intensity Factor K from Isochromatic Fringe Loops," Engineering Fracture Mechanics, Vol. 10, No. 1, 1978, pp. 81-93.

17. William, M. L. "On the Stress Distribution at the Base of a Stationary Crack," Journal of Applied Mechanics, Trans. of ASME, Vol. 24, No. 2, 1976, pp. 109-114.

18. Kobayashi, A. S. and Mall, S., "Dynamic Fracture Toughness of Homalite-100," Experimental Mechanics, Vol 18, No. 1, Jan. 1978, pp. 11-18.

19. King, W. W., Malluck, J. F., Aberson, J. A., and Anderson, J. M., "Application of Running Crack Eigenfunction to Finite Element Simulation of Crack Propagation," Mechanics Research Communication, Vol. 3, No. 3, 1976, pp. 197-202.

20. Kobayashi, A. S., Wade, B. G. and Maiden, D. E., "An Investigation on the Crack Arrest Capability of a Hole," Experimental Mechanics, Vol. 12, No. 1, Jan. 1972, pp. 32-37.

21. Irwin, G. R., Dally, J. W., Kobayashi, T., Fourney, W. L. and Ethridge, J. M., "A Photoelastic Characterization of Dynamic Fracture," a University of Maryland report prepared under U. S. Nuclear Regulatory Commission Contract AT(49-23)-0172, NUREG-0072, Dec. 1976.

22. Hodulak, L., Kobayashi, A. S. and Emery, A. F., "A Critical Examination of a Numerical Fracture Dynamic Code," a paper submitted for presentation at the ASTM 12th Annual Symposium on Fracture Mechanics.

23. Kobayashi, A. S., Emery, A. F. and Mall, S., "Dynamic Finite Element and Dynamic Photoelastic Analyses of Two-Fracturing Homalite-100 Plates," Experimental Mechanics, Vol. 16, No. 9, Sept. 1976, pp. 321-328.

24. Schirrer, R., "The Effects of a Strain Rate-Dependent Young's Modulus upon the Stress and Strain Fields Around a Running Crack Tip", International Journal of Fracture, Vol. 14, No. 3, June 1978, pp. 265-279.

25. Kalthoff, J., Beinert, J. and Winkler, S., "Experimental Analysis of Dynamic Effects in Different Crack Arrest Specimens," a paper presented at the ASTM E-24 Symposium Crack Arrest Methodology and Applications, Philadelphia, Nov. 6-7, 1973.

26. Hodulak, L., Kobayashi, A. S. and Emergy, A. F., "Influence of Dynamic Fracture Toughness on Dynamic Crack Propagation" submitted to ASME Journal of Pressure Vessel Technology.

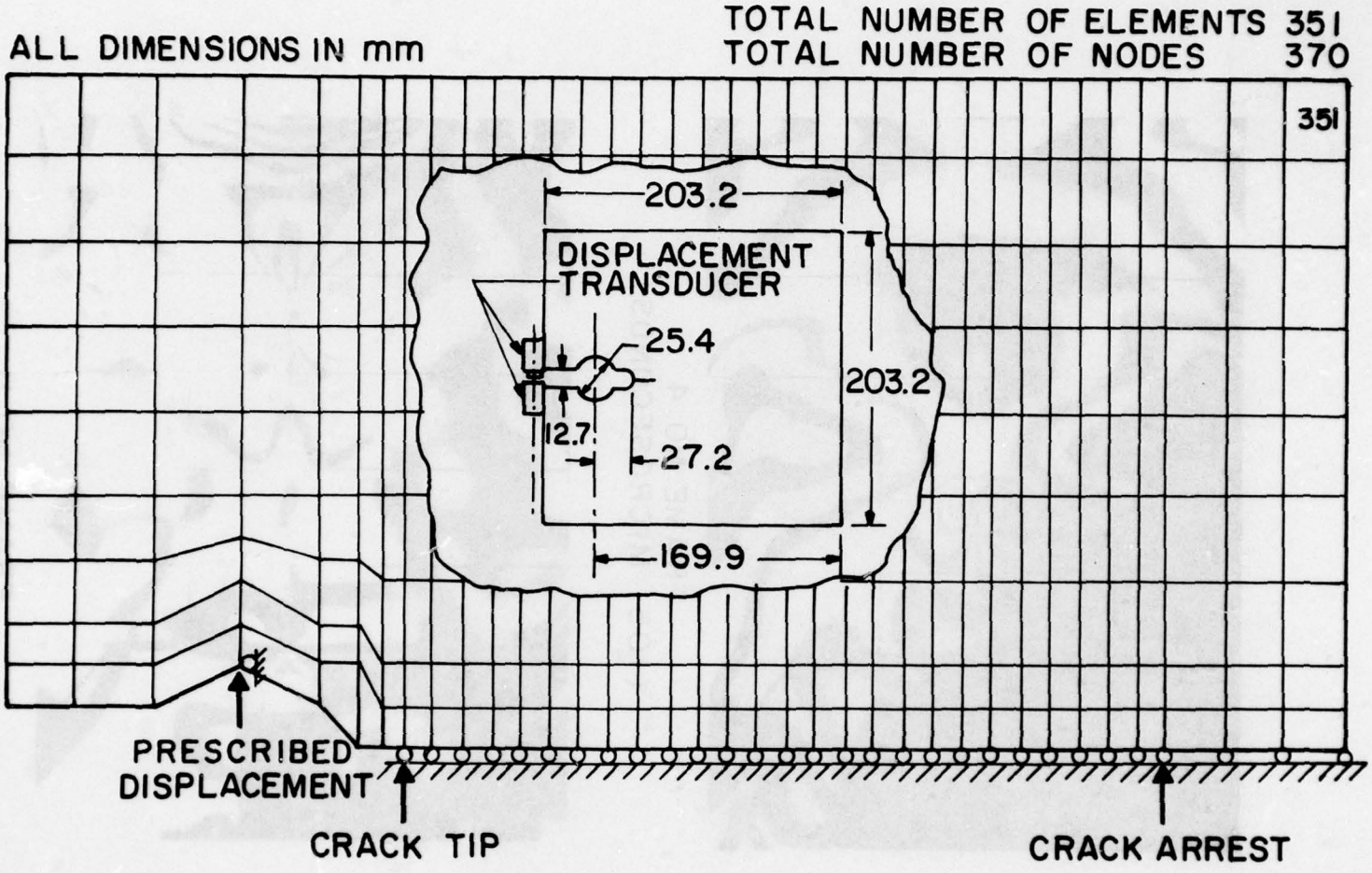

FIGURE 1. TYPICAL FINITE ELEMENT BREAKDOWN OF M-CT SPECIMEN.

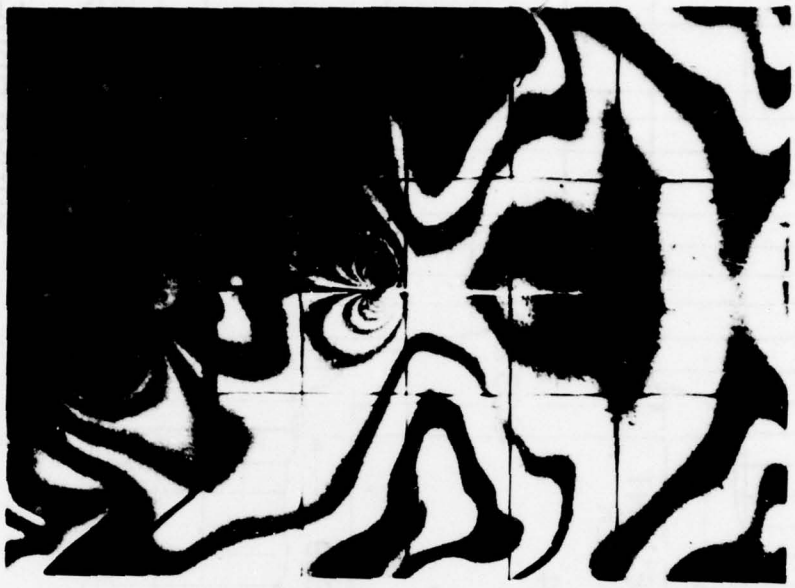

FRAME NO. 4
(105 MICROSECONDS)

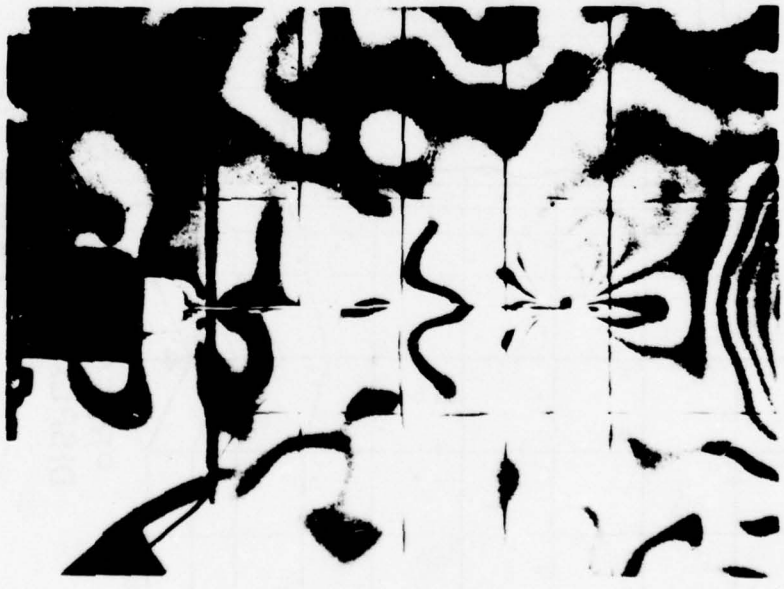

FRAME NO. 11
(307 MICROSECONDS)

FIGURE 2. TYPICAL DYNAMIC PHOTOELASTIC FRINGES IN A FRACTURING POLYCARBONATE M-CT SPECIMEN, J280678.

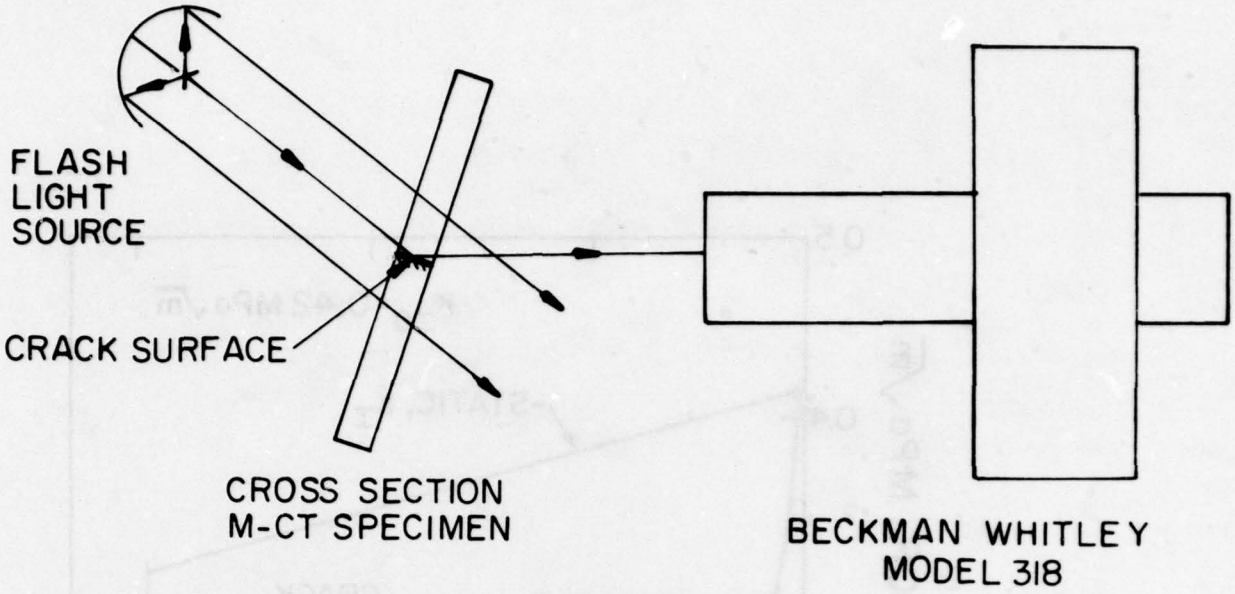

EXPERIMENTAL SET UP FOR STREAKING PHOTOGRAPHY

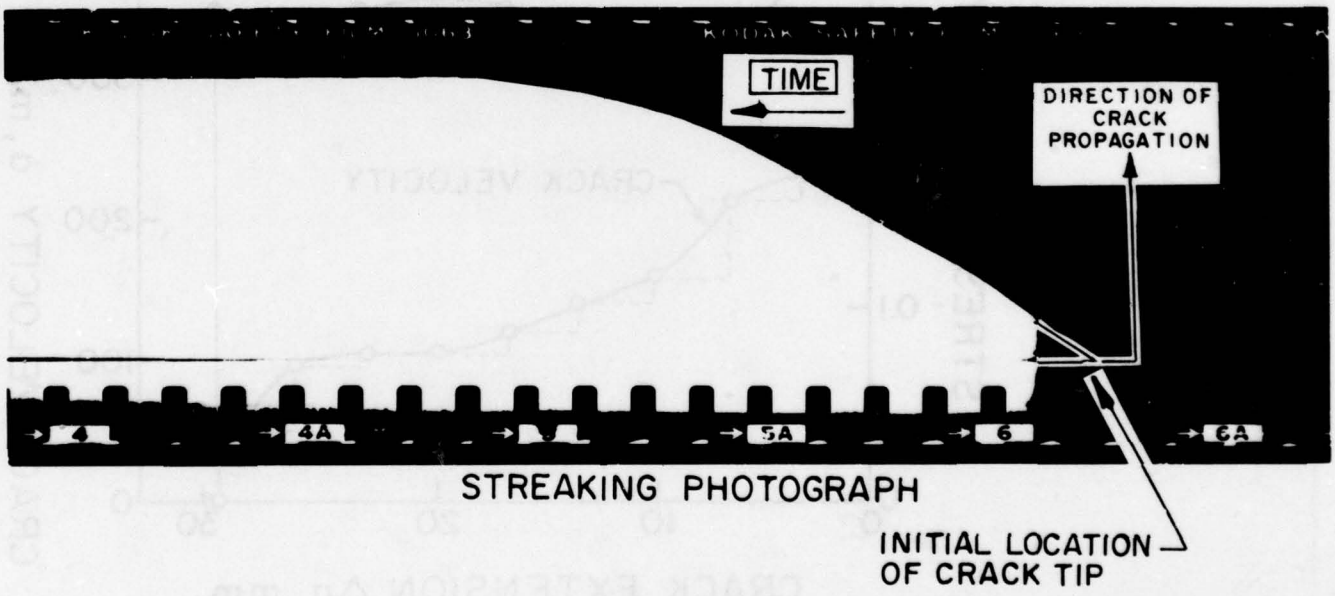

FIGURE 3. STREAKING PHOTOGRAPH OF A PROPAGATING CRACK TIP IN A POLYCARBONATE M-CT SPECIMEN (THICKNESS 6.4mm).

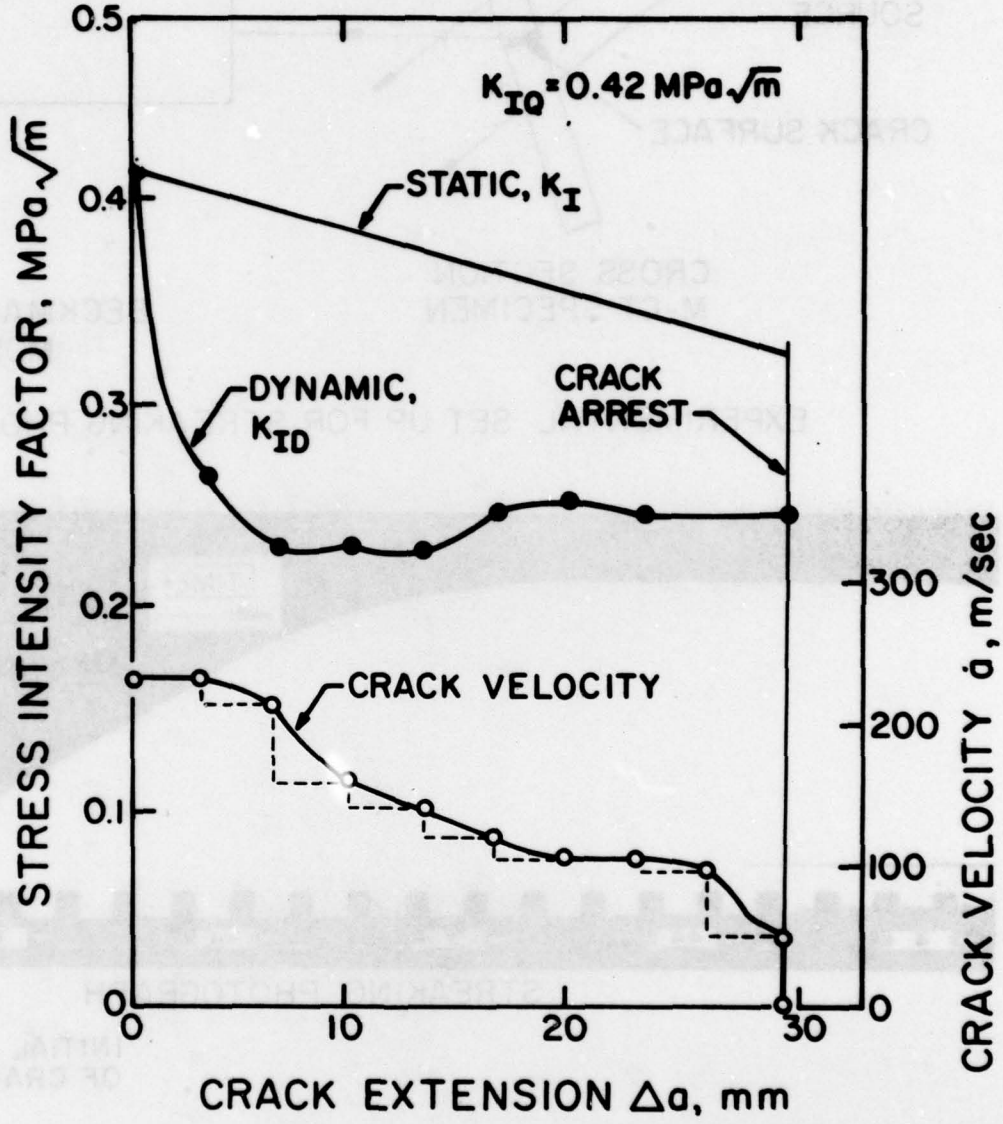

FIGURE 4. CRACK VELOCITY AND STRESS INTENSITY FACTORS OF A FRACTURING HOMALITE-100 M-CT SPECIMEN. S100277 (PRECRACKED)

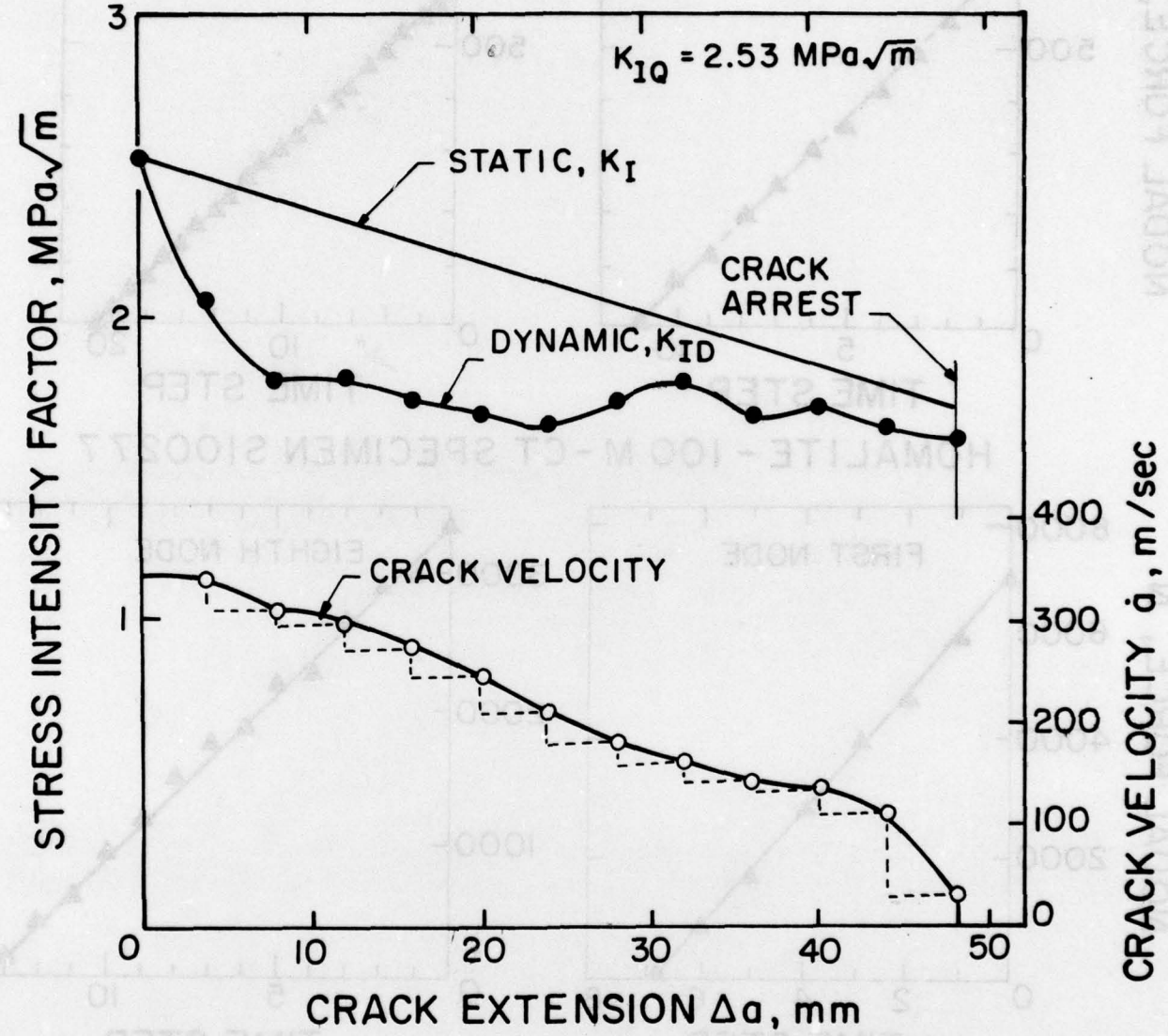

FIGURE 5. DYNAMIC FRACTURE TOUGHNESS AND CRACK VELOCITY OF A FRACTURING POLYCARBONATE M-CT SPECIMEN. S100377 (PRECRACKED).

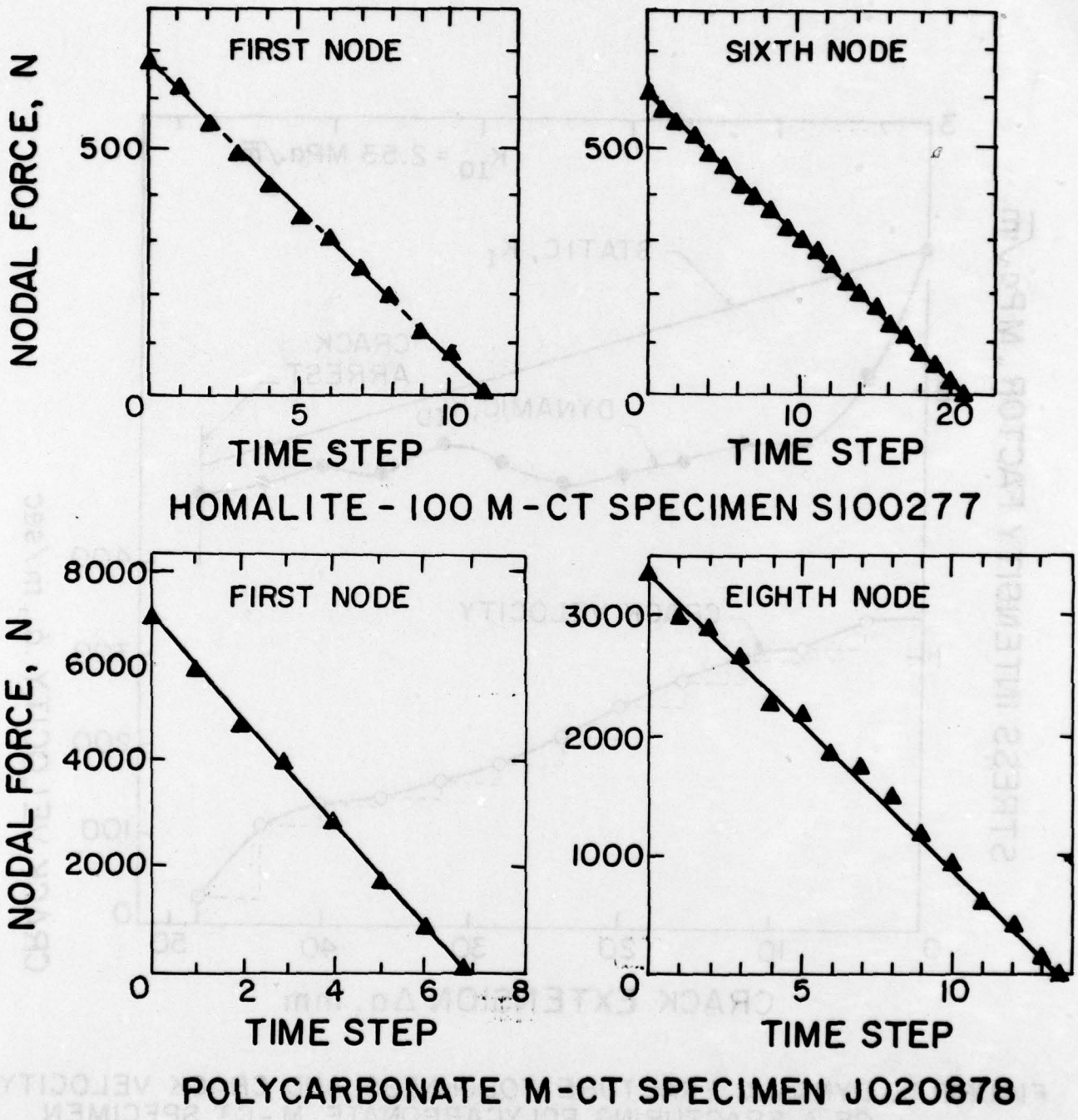

FIGURE 6. TYPICAL COMPUTED NODAL FORCE RELEASED.

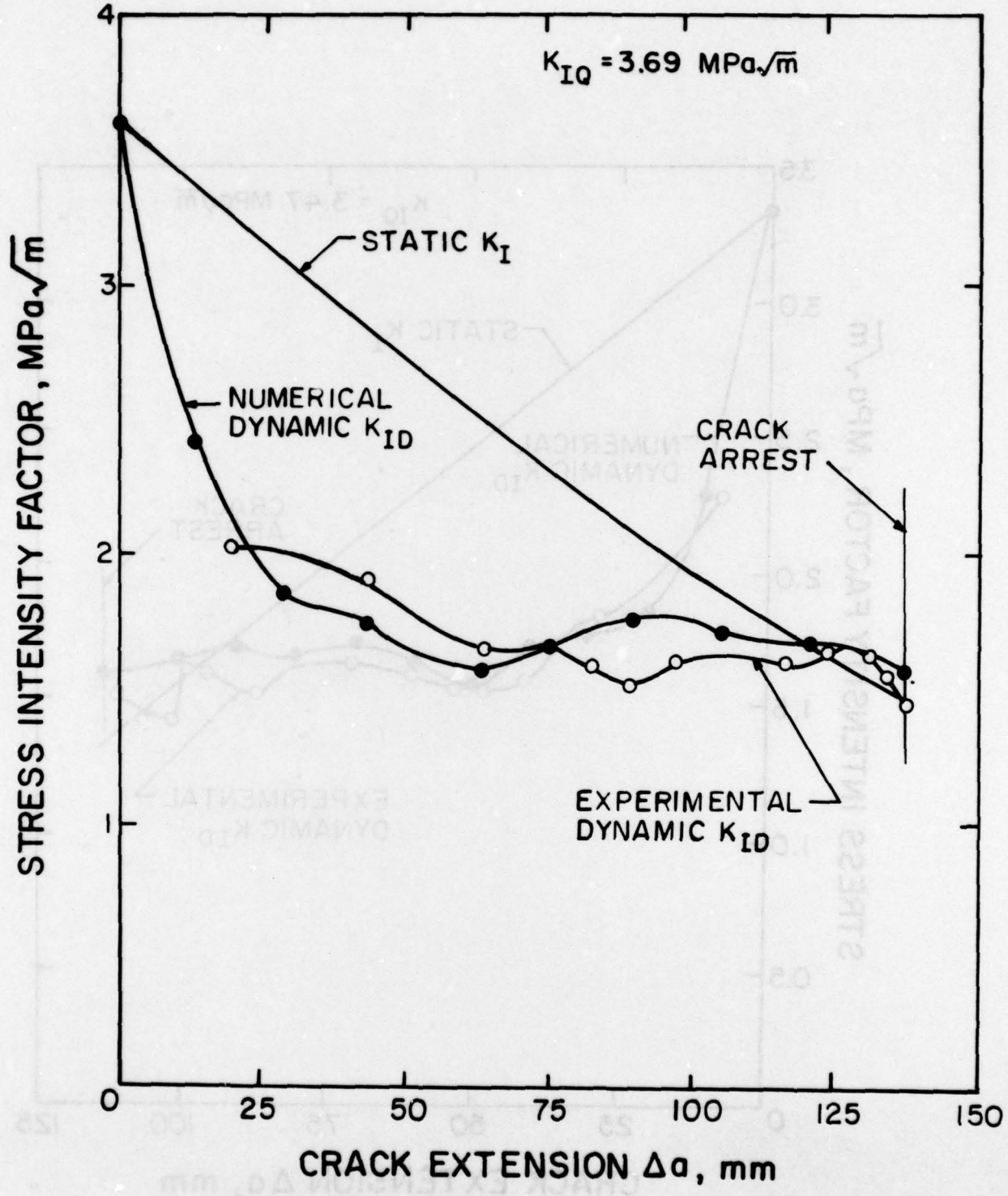

FIGURE 7. STRESS INTENSITY FACTORS OF A FRACTURING POLY-CARBONATE M-CT SPECIMEN, J-280678.

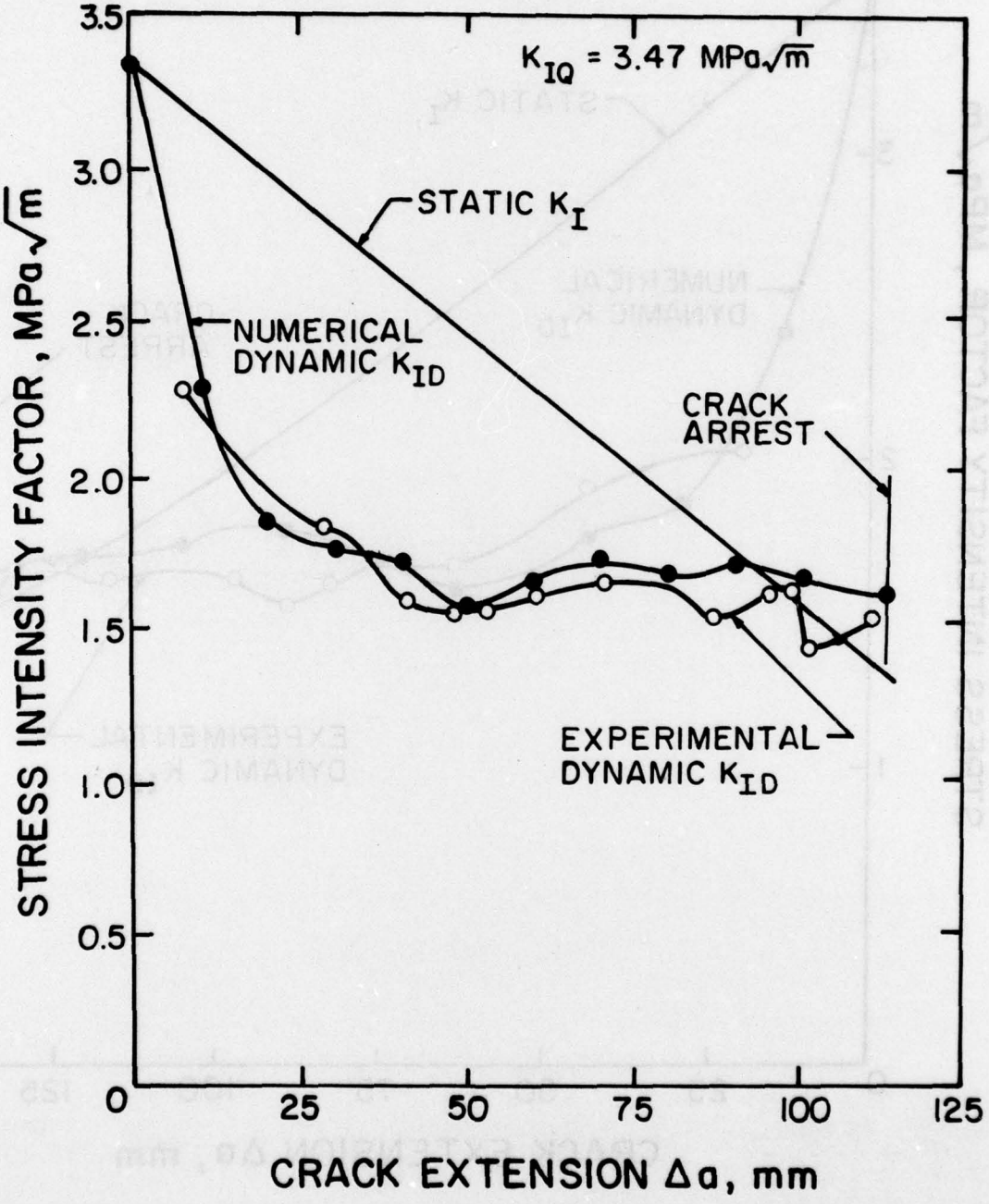

FIGURE 8. STRESS INTENSITY FACTORS OF A FRACTURING POLYCARBONATE M-CT SPECIMEN, J-020878.

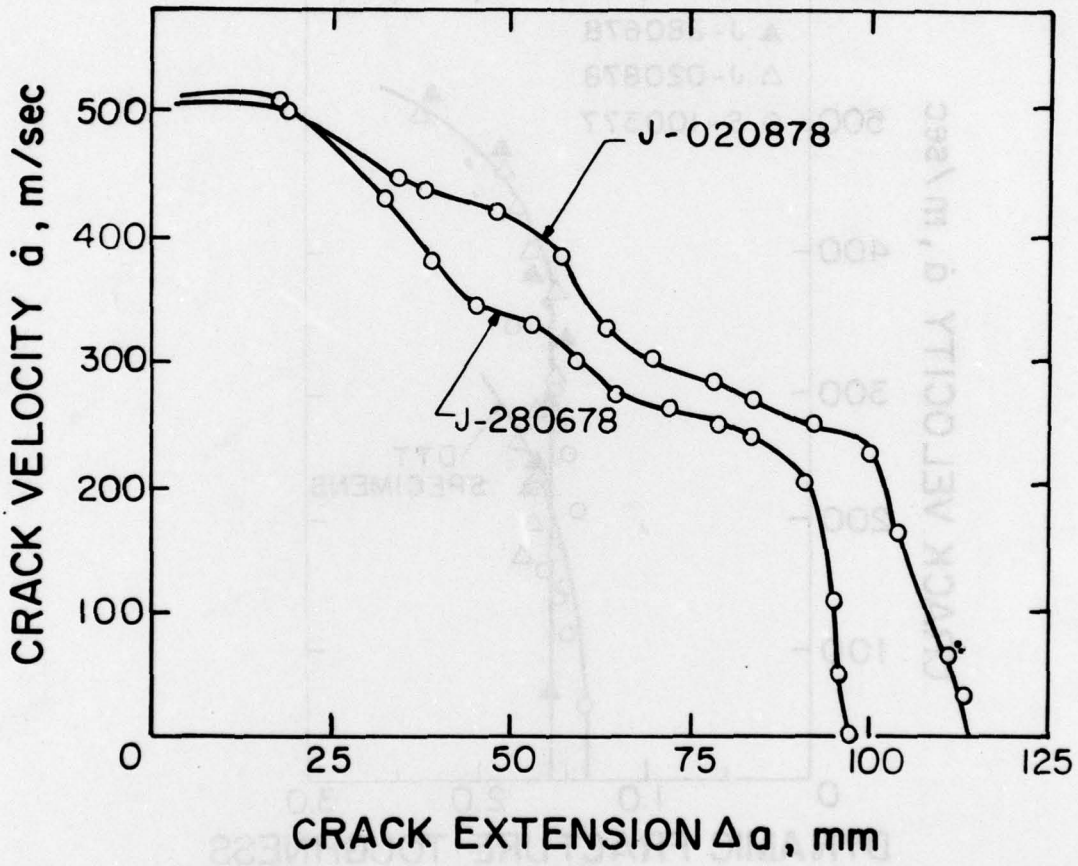

FIGURE 9. CRACK VELOCITIES IN TWO FRACTURING POLYCARBONITE M-CT SPECIMENS.

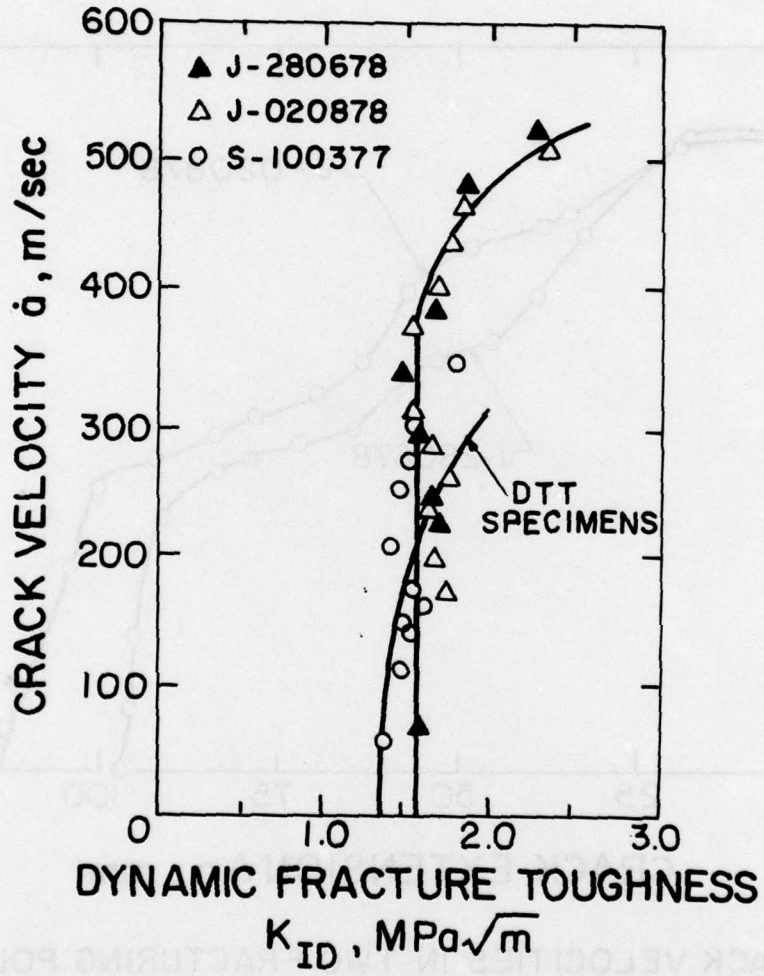

FIGURE 10. DYNAMIC FRACTURE TOUGHNESS VERSUS CRACK VELOCITY RELATION FOR POLY-CARBONATE SPECIMEN.

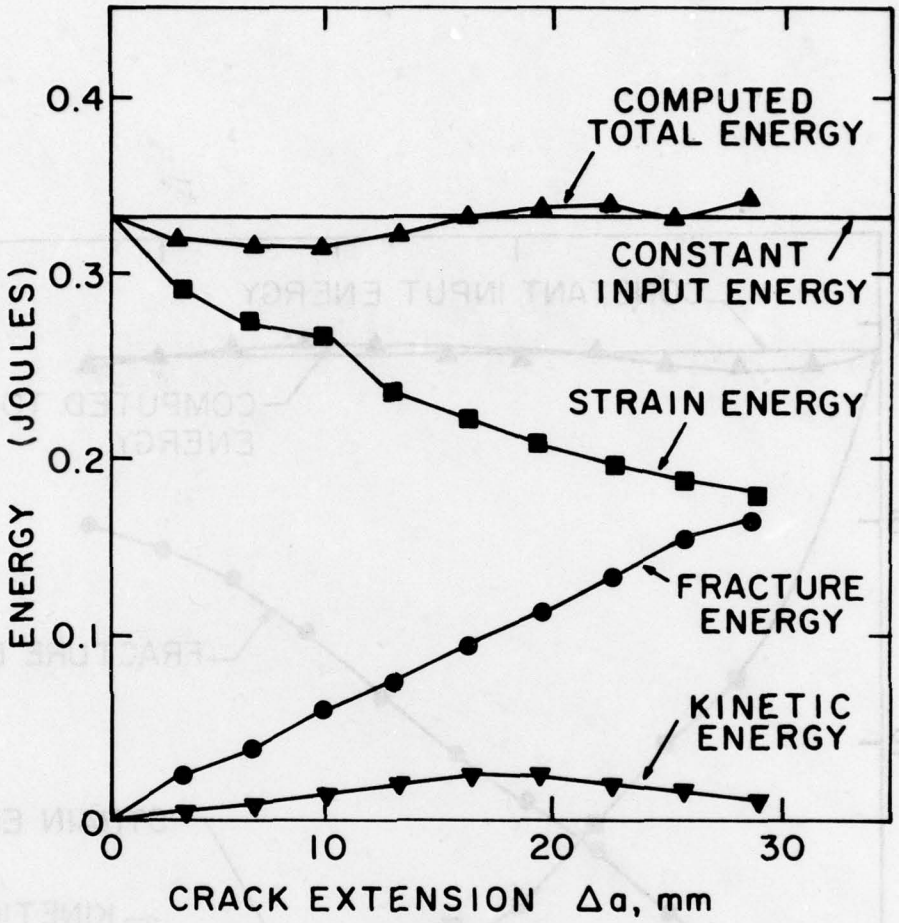

FIGURE 11. ENERGY OF A FRACTURING HOMALITE - 100 M-CT SPECIMEN, S100277.

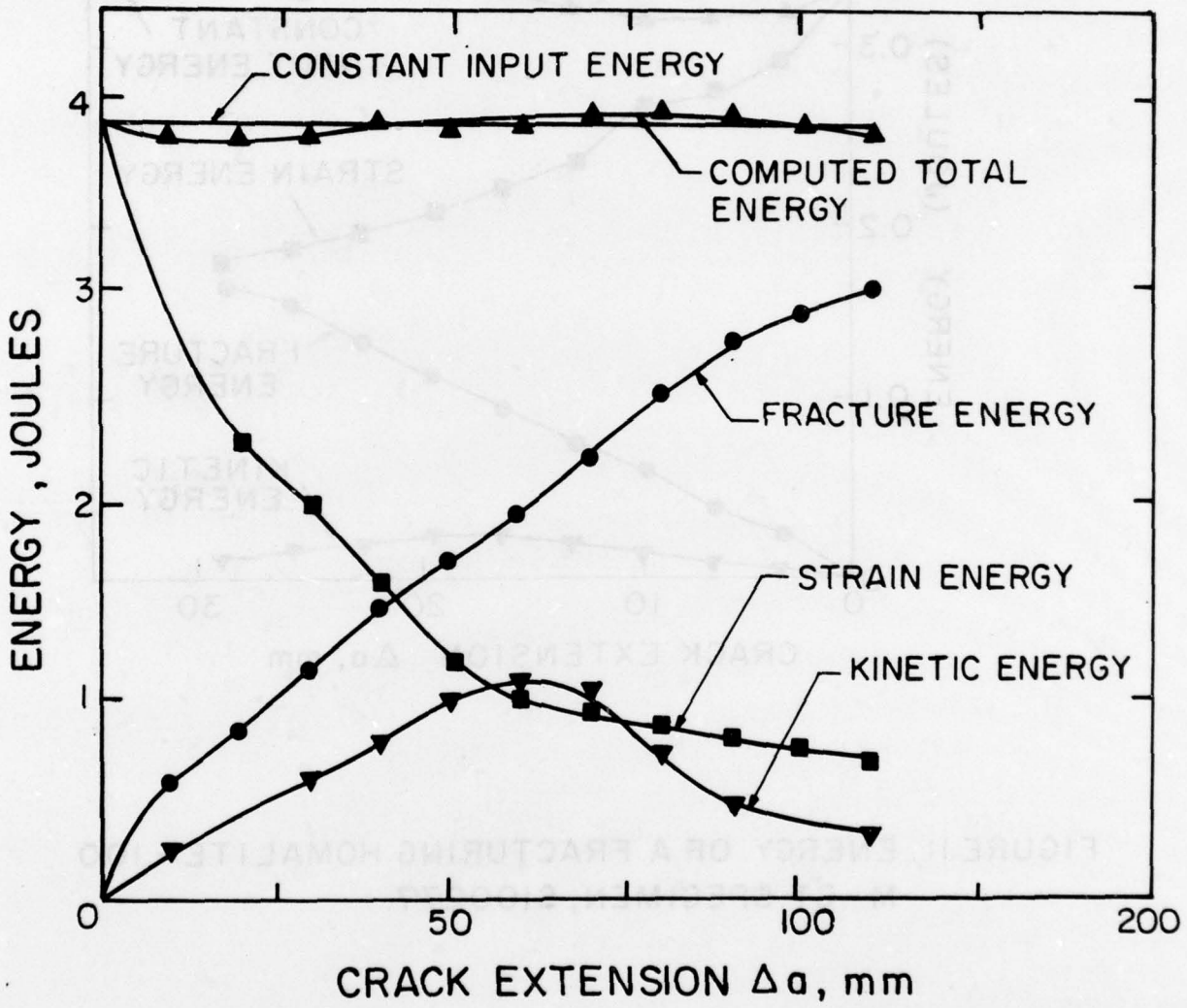

FIGURE 12. ENERGY OF A FRACTURING POLYCARBONATE M-CT SPECIMEN, J-020878.

PART 1 - Government

Administrative and Liaison Activities

Office of Naval Research
Department of the Navy
Arlington, VA 22217
Attn: Code 474 (2)
Code 471
Code 200

Director
Office of Naval Research
Branch Office
666 Summer Street
Boston, MA 02210

Director
Office of Naval Research
Branch Office
536 South Clark Street
Chicago, IL 60605

Director
Office of Naval Research
New York Area Office
715 Broadway - 5th Floor
New York, NY 10003

Director
Office of Naval Research
Branch Office
1030 East Green Street
Pasadena, CA 91106

Naval Research Laboratory (6)
Code 2627
Washington, DC 20375

Defense Documentation Center (12)
Cameron Station
Alexandria, VA 22314

Navy

Undersea Explosion Research Division
Naval Ship Research and Development Center
Norfolk Naval Shipyard
Portsmouth, VA 23709
Attn: Dr. E. Palmer, Code 177

Navy (Con't.)

Naval Research Laboratory
Washington, DC 20375
Attn: Code 8400
8410
8430
8440
6300
6390
6380

David W. Taylor Naval Ship Research and Development Center
Annapolis, MD 21402
Attn: Code 2740
28
281

U.S. Naval Weapons Center
China Lake, CA 93555
Attn: Code 4062
4520

Commanding Officer
U.S. Naval Civil Engineering Laboratory
Code L31
Port Hueneme, CA 93041

Naval Surface Weapons Center
White Oak
Silver Spring, MD 20910
Attn: Code R-10
G-402
K-82

Technical Director
Naval Ocean Systems Center
San Diego, CA 92152

Supervisor of Shipbuilding
U.S. Navy
Newport News, VA 23607

U.S. Navy Underwater Sound Reference Division
Naval Research Laboratory
P.O. Box 8337
Orlando, FL 32806

Navy (Con't.)

Chief of Naval Operations
Department of the Navy
Washington, DC 20350
Attn: Code OP-098

Strategic Systems Project Office
Department of the Navy
Washington, DC 20376
Attn: NSP-200

Naval Air Systems Command
Department of the Navy
Washington, DC 20361
Attn: Code 5302 (Aerospace and Structures)
604 (Technical Library)
320B (Structures)

Naval Air Development Center
Director, Aerospace Mechanics
Warminster, PA 18974

U.S. Naval Academy
Engineering Department
Annapolis, MD 21402

Naval Facilities Engineering Command
200 Stovall Street
Alexandria, VA 22332
Attn: Code 03 (Research and Development)
04B
045
14114 (Technical Library)

Naval Sea Systems Command
Department of the Navy
Washington, DC 20362
Attn: Code 03 (Research and Technology)
037 (Ship Silencing Division)
035 (Mechanics and Materials)

Naval Ship Engineering Center
Department of the Navy
Washington, DC 20362
Attn: Code 6105G
6114
6120D
6128
6129

Commanding Officer and Director
David W. Taylor Naval Ship Research and Development Center
Bethesda, MD 20084
Attn: Code 042
17
172
173
174
1800
1844
1102.1
1900
1901
1945
1960
1962

Naval Underwater Systems Center
Newport, RI 02840
Attn: Dr. R. Trainor

Naval Surface Weapons Center
Dahlgren Laboratory
Dahlgren, VA 22448
Attn: Code G04
G20

Technical Director
Mare Island Naval Shipyard
Vallejo, CA 94592

U.S. Naval Postgraduate School
Library
Code 0384
Monterey, CA 93940

Webb Institute of Naval Architecture
Attn: Librarian
Crescent Beach Road, Glen Cove
Long Island, NY 11542

Army

Commanding Officer (2)
U.S. Army Research Office
P.O. Box 12211
Research Triangle Park, NC 27709
Attn: Mr. J. J. Murray, CRD-AA-IP

Watervliet Arsenal
MAGGS Research Center
Watervliet, NY 12189
Attn: Director of Research

U.S. Army Materials and Mechanics Research Center
Watertown, MA 02172
Attn: Dr. R. Shea, DRXMR-T

U.S. Army Missile Research and Development Center
Redstone Scientific Information Center
Chief, Document Section
Redstone Arsenal, AL 35809

Army Research and Development Center
Fort Belvoir, VA 22060

NASA

National Aeronautics and Space Administration
Structures Research Division
Langley Research Center
Langley Station
Hampton, VA 23365

National Aeronautics and Space Administration
Associate Administrator for Advanced Research and Technology
Washington, DC 20546

Scientific and Technical Information Facility
NASA Representative (S-AK/DL)
P.O. Box 5700
Bethesda, MD 20014

Air Force

Commander WADD
Wright-Patterson Air Force Base
Dayton, OH 45433
Attn: Code WWRMDD
AFFDL (FDDS)
Structures Division
AFLC (MCEEA)

Chief Applied Mechanics Group
U.S. Air Force Institute of Technology
Wright-Patterson Air Force Base
Dayton, OH 45433

Chief, Civil Engineering Branch
WLRC, Research Division
Air Force Weapons Laboratory
Kirtland Air Force Base
Albuquerque, NM 87117

Air Force Office of Scientific Research
Bolling Air Force Base
Washington, DC 20332
Attn: Mechanics Division

Department of the Air Force
Air University Library
Maxwell Air Force Base
Montgomery, AL 36112

Other Government Activities

Commandant
Chief, Testing and Development Division
U.S. Coast Guard
1300 E Street, NW
Washington, DC 20226

Technical Director
Marine Corps Development and Education Command
Quantico, VA 22134

Director Defense Research and Engineering
Technical Library
Room 3C128
The Pentagon
Washington, DC 20301

Director
National Bureau of Standards
Washington, DC 20034
Attn: Mr. B. L. Wilson, EM 219

Dr. M. Gaus
National Science Foundation
Environmental Research Division
Washington, DC 20550

Library of Congress
Science and Technology Division
Washington, DC 20540

Director
Defense Nuclear Agency
Washington, DC 20305
Attn: SPSS

Mr. Jerome Persh
Staff Specialist for Materials and Structures
OUSDR&E, The Pentagon
Room 3D1089
Washington, DC 20301

Chief, Airframe and Equipment Branch
FS-120
Office of Flight Standards
Federal Aviation Agency
Washington, DC 20553

National Academy of Sciences
National Research Council
Ship Hull Research Committee
2101 Constitution Avenue
Washington, DC 20418
Attn: Mr. A. R. Lytle

National Science Foundation
Engineering Mechanics Section
Division of Engineering
Washington, DC 20550

Picatinny Arsenal
Plastics Technical Evaluation Center
Attn: Technical Information Section
Dover, NJ 07801

Maritime Administration
Office of Maritime Technology
14th and Constitution Ave., NW
Washington, DC 20230

Maritime Administration
Office of Ship Construction
14th and Constitution Ave., NW
Washington, DC 20230

PART 2 - Contractors and Other Technical Collaborators

Universities

Dr. J. Tinsley Oden
University of Texas at Austin
345 Engineering Science Building
Austin, TX 78712

Professor Julius Miklowitz
California Institute of Technology
Division of Engineering
and Applied Sciences
Pasadena, CA 91109

Dr. Harold Liebowitz, Dean
School of Engineering and
Applied Science
George Washington University

Professor Eli Sternberg
California Institute of Technology
Division of Engineering and
Applied Sciences
Pasadena, CA 91109

Professor Paul M. Naghdi
University of California
Department of Mechanical Engineering
Berkeley, CA 94720

Professor A. J. Durelli
Oakland University
School of Engineering
Rochester, MI 48063

Professor F. L. DiMaggio
Columbia University
Department of Civil Engineering
New York, NY 10027

Professor Norman Jones
Massachusetts Institute of Technology
Department of Ocean Engineering
Cambridge, MA 02139

Professor E. J. Skudrzyk
Pennsylvania State University
Applied Research Laboratory
Department of Physics
State College, PA 16801

Professor J. Kempner
Polytechnic Institute of New York
Department of Aerospace Engineering and
Applied Mechanics
333 Jay Street
Brooklyn, NY 11201

Professor J. Klosner
Polytechnic Institute of New York
Department of Aerospace Engineering and
Applied Mechanics
333 Jay Street
Brooklyn, NY 11201

Professor R. A. Schapery
Texas A&M University
Department of Civil Engineering
College Station, TX 77843

Professor Walter D. Pilkey
University of Virginia
Research Laboratories for the
Engineering Sciences
School of Engineering and
Applied Sciences
Charlottesville, VA 22901

Professor K. D. Willmert
Clarkson College of Technology
Department of Mechanical Engineering
Potsdam, NY 13676

Dr. Walter E. Haisler
Texas A&M University
Aerospace Engineering Department
College Station, TX 77843

Dr. Hussein A. Kamel
University of Arizona
Department of Aerospace and
Mechanical Engineering
Tucson, AZ 85721

Dr. S. J. Fenves
Carnegie-Mellon University
Department of Civil Engineering
Schenley Park
Pittsburgh, PA 15213

Universities (Con't.)

Professor H. W. Liu
Syracuse University
Department of Chemical Engineering
and Metallurgy
Syracuse, NY 13210

Professor S. Bodner
Technion R&D Foundation
Haifa, Israel

Professor Werner Goldsmith
University of California
Department of Mechanical Engineering
Berkeley, CA 94720

Professor R. S. Rivlin
Lehigh University
Center for the Application
of Mathematics
Bethlehem, PA 18015

Professor F. A. Cozzarelli
State University of New York at Buffalo
Division of Interdisciplinary Studies
Karr Parker Engineering Building
Chemistry Road
Buffalo, NY 14214

Professor Joseph L. Rose
Drexel University
Department of Mechanical Engineering
and Mechanics
Philadelphia, PA 19104

Professor B. K. Donaldson
University of Maryland
Aerospace Engineering Department
College Park, MD 20742

Professor Joseph A. Clark
Catholic University of America
Department of Mechanical Engineering
Washington, DC 20064

Professor T. C. Huang
University of Wisconsin-Madison
Department of Engineering Mechanics
Madison, WI 53706

Dr. Samuel B. Batdorf
University of California
School of Engineering
and Applied Science
Los Angeles, CA 90024

Professor Isaac Fried
Boston University
Department of Mathematics
Boston, MA 02215

Professor Michael Pappas
New Jersey Institute of Technology
Newark College of Engineering
323 High Street
Newark, NJ 07102

Professor E. Krempl
Rensselaer Polytechnic Institute
Division of Engineering
Engineering Mechanics
Troy, NY 12181

Dr. Jack R. Vinson
University of Delaware
Department of Mechanical and Aerospace
Engineering and the Center for
Composite Materials
Newark, DL 19711

Dr. Dennis A. Nagy
Princeton University
School of Engineering and Applied Science
Department of Civil Engineering
Princeton, NJ 08540

Dr. J. Duffy
Brown University
Division of Engineering
Providence, RI 02912

Dr. J. L. Swedlow
Carnegie-Mellon University
Department of Mechanical Engineering
Pittsburgh, PA 15213

Dr. V. K. Varadan
Ohio State University Research Foundation
Department of Engineering Mechanics
Columbus, OH 43210

Universities (Con't.)

Dr. Ronald L. Huston
Department of Engineering Analysis
University of Cincinnati
Cincinnati, OH 45221

Professor G. C. M. Sih
Lehigh University
Institute of Fracture and
Solid Mechanics
Bethlehem, PA 18015

Professor Albert S. Kobayashi
University of Washington
Department of Mechanical Engineering
Seattle, WA 98105

Professor Daniel Frederick
Virginia Polytechnic Institute and
State University
Department of Engineering Mechanics
Blacksburg, VA 24061

Professor A. C. Eringen
Princeton University
Department of Aerospace and
Mechanical Sciences
Princeton, NJ 08540

Professor E. H. Lee
Stanford University
Division of Engineering Mechanics
Stanford, CA 94305

Professor Albert I. King
Wayne State University
Biomechanics Research Center
Detroit, MI 48202

Dr. V. R. Hodgson
Wayne State University
School of Medicine
Detroit, MI 48202

Dean B. A. Boley
Northwestern University
Department of Civil Engineering
Evanston, IL 60201

Professor P. G. Hodge, Jr.
University of Minnesota
Department of Aerospace Engineering
and Mechanics
Minneapolis, MN 55455

Dr. D. C. Drucker
University of Illinois
Dean of Engineering
Urbana, IL 61801

Professor N. M. Newmark
University of Illinois
Department of Civil Engineering
Urbana, IL 61803

Professor E. Reissner
University of California, San Diego
Department of Applied Mechanics
La Jolla, CA 92037

Professor William A. Nash
University of Massachusetts
Department of Mechanics and
Aerospace Engineering
Amherst, MA 01002

Professor G. Herrmann
Stanford University
Department of Applied Mechanics
Stanford, CA 94305

Professor J. D. Achenbach
Northwestern University
Department of Civil Engineering
Evanston, IL 60201

Professor S. B. Dong
University of California
Department of Mechanics
Los Angeles, CA 90024

Professor Burt Paul
University of Pennsylvania
Towne School of Civil and
Mechanical Engineering
Philadelphia, PA 19104

Universities (Con't.)

Dr. Z. Hashin
University of Pennsylvania
Department of Metallurgy and
Materials Science
College of Engineering and
Applied Science
Philadelphia, PA 19104

Dr. Jackson C. S. Yang
University of Maryland
Department of Mechanical Engineering
College Park, MD 20742

Professor T. Y. Chang
University of Akron
Department of Civil Engineering
Akron, OH 44325

Professor Charles W. Bert
University of Oklahoma
School of Aerospace, Mechanical,
and Nuclear Engineering
Norman, OK 73019

Professor Satya N. Atluri
Georgia Institute of Technology
School of Engineering Science and
Mechanics
Atlanta, GA 30332

Professor Graham F. Carey
University of Texas at Austin
Department of Aerospace Engineering
and Engineering Mechanics
Austin, TX 78712

Industry and Research Institutes

Dr. Jackson C. S. Yang
Advanced Technology and Research, Inc.
10006 Green Forest Drive
Adelphi, MD 20783

Dr. Norman Hobbs
Kaman AviDyne
Division of Kaman
Sciences Corp.
Burlington, MA 01803

Industry and Research Institutes (Con't.)

Argonne National Laboratory
Library Services Department
9700 South Cass Avenue
Argonne, IL 60440

Dr. M. C. Junger
Cambridge Acoustical Associates
1033 Massachusetts Avenue
Cambridge, MA 02138

Dr. V. Godino
General Dynamics Corporation
Electric Boat Division
Groton, CT 06340

Dr. J. E. Greenspon
J. G. Engineering Research Associates
3831 Menlo Drive
Baltimore, MD 21215

Dr. K. C. Park
Lockheed Missile and Space Company
3251 Hanover Street
Palo Alto, CA 94304

Newport News Shipbuilding and
Dry Dock Company
Library
Newport News, VA 23607

Dr. W. F. Bozich
McDonnell Douglas Corporation
5301 Bolsa Avenue
Huntington Beach, CA 92647

Dr. H. N. Abramson
Southwest Research Institute
8500 Culebra Road
San Antonio, TX 78284

Dr. R. C. DeHart
Southwest Research Institute
8500 Culebra Road
San Antonio, TX 78284

Dr. M. L. Baron
Weidlinger Associates
110 East 59th Street
New York, NY 10022

Industry and Research Institutes (Con't.)

Dr. T. L. Geers
Lockheed Missiles and Space Company
3251 Hanover Street
Palo Alto, CA 94304

Mr. William Caywood
Applied Physics Laboratory
Johns Hopkins Road
Laurel, MD 20810

Dr. Robert E. Nickell
Pacifica Technology
P.O. Box 148
Del Mar, CA 92014

Dr. M. F. Kanninen
Battelle Columbus Laboratories
505 King Avenue
Columbus, OH 43201

Dr. G. T. Hahn
Battelle Columbus Laboratories
505 King Avenue
Columbus, OH 43201

Dr. A. A. Hochrein
Daedalean Associates, Inc.
Springlake Research Center
15110 Frederick Road
Woodbine, MD 21797

Mr. Richard Y. Dow
National Academy of Sciences
2101 Constitution Avenue
Washington, DC 20418

Mr. H. L. Kington
Airesearch Manufacturing Company
of Arizona
P.O. Box 5217
111 South 34th Street
Phoenix, AZ 85010

Dr. M. H. Rice
Systems, Science, and Software
P.O. Box 1620
La Jolla, CA 92037

Unclassified

SECURITY CLASSIFICATION OF THIS PAGE (When Data Entered)

REPORT DOCUMENTATION PAGE

READ INSTRUCTIONS BEFORE COMPLETING FORM

1. REPORT NUMBER: TR 35
2. GOVT ACCESSION NO.:
3. RECIPIENT'S CATALOG NUMBER:

4. TITLE (and Subtitle): Dynamic Analyses of Homalite-100 and Polycarbonate Modified Compact-Tension Specimens.
5. TYPE OF REPORT & PERIOD COVERED: Technical Report
6. PERFORMING ORG. REPORT NUMBER: TR-35

7. AUTHOR(s): A.S. Kobayashi, K. Seo, J.Y. Jou, Y. Urabe
8. CONTRACT OR GRANT NUMBER(s): N00014-76-C-0060

9. PERFORMING ORGANIZATION NAME AND ADDRESS:
Dept. of Mechanical Engineering, FU-10
University of Washington
Seattle, Washington 98195

10. PROGRAM ELEMENT, PROJECT, TASK AREA & WORK UNIT NUMBERS: NR 064-478

11. CONTROLLING OFFICE NAME AND ADDRESS:
Office of Naval Research
Arlington, Virginia 22217

12. REPORT DATE: March 1979
13. NUMBER OF PAGES: 25

14. MONITORING AGENCY NAME & ADDRESS (if different from Controlling Office):

15. SECURITY CLASS. (of this report): Unclassified
15a. DECLASSIFICATION/DOWNGRADING SCHEDULE:

16. DISTRIBUTION STATEMENT (of this Report)

Unlimited

17. DISTRIBUTION STATEMENT (of the abstract entered in Block 20, if different from Report)

18. SUPPLEMENTARY NOTES

19. KEY WORDS (Continue on reverse side if necessary and identify by block number)
Dynamic fracture toughness, crack arrest toughness, dynamic fracture mechanics, dynamic finite element analysis

20. ABSTRACT (Continue on reverse side if necessary and identify by block number)

The fracture dynamic and crack arrest responses of modified compact tension specimen (M-CT) machined from Homalite-100 and polycarbonate sheets were studied by dynamic photoelasticity, dynamic finite element analysis and streaking photography. In contrast to the results of a previous study involving a mild steel M-CT specimen, substantial dynamic effects were observed during crack propagation in the Homalite-100 and polycarbonate M-CT specimens. Although the crack arrest toughnesses, K_{Ia}, were within

DD FORM 1 JAN 73 1473 EDITION OF 1 NOV 65 IS OBSOLETE
S/N 0102-014-6601

Unclassified
SECURITY CLASSIFICATION OF THIS PAGE (When Data Entered)

400 344

JOB

10 percent of the corresponding static stress intensity factor at crack arrest, their values were about 80 percent and 50 percent of the corresponding fracture toughness, K_{IC}, of Homalite-100 and polycarbonate, respectively.